A General-Purpose Multi-Modal OOD Detection Framework

Anonymous authors
Paper under double-blind review

Abstract

Out-of-distribution (OOD) detection seeks to identify test samples that deviate from the training data, which is critical to ensuring the safety and reliability of machine learning (ML) systems. While a plethora of methods have been developed to detect uni-modal OOD samples, only a few have focused on multi-modal OOD detection. Current contrastive learning-based methods primarily address multi-modal OOD detection in a scenario where an image is not related to the class labels in training data. However, ML systems in the real-world applications may encounter a broader spectrum of anomalies caused by different factors like systematic errors in labeling, environmental changes, and sensor malfunctions. Hence, we propose a new method to be able to simultaneously detect anomalies from multiple different OOD scenarios, arising from fine-grained image features and textual descriptions, instead of large categorical information. To achieve this goal, we propose a general-purpose weakly-supervised OOD detection framework, called WOOD, that combines a binary classifier and a contrastive learning module to reap the benefits of both. In order to better distinguish in-distribution (ID) samples from OOD ones, we employ the Hinge loss to constrain the similarity of their latent representations. Moreover, we devise a new scoring metric that fuses predictions from both the binary classifier and contrastive learning to enhance OOD detection. Extensive experimental results on multiple benchmarks demonstrate that the proposed WOOD significantly outperforms the state-of-the-art methods for multi-modal OOD detection. Importantly, our approach can achieve superior detection performance in a variety of OOD scenarios. The source code will be made publicly available upon publication.

1 Introduction

Out-of-distribution (OOD) detection (Yang et al., 2021; Bogdoll et al., 2022; Ming et al., 2022c; Ruff et al., 2021; Ma et al., 2021) aims at identifying whether a test sample differs from the training data. Such detection is crucial for ensuring the safety and reliability of machine learning (ML) systems (Wang et al., 2020; Hussain & Zeadally, 2018), such as autonomous driving and AI diagnosis (Davenport & Kalakota, 2019; Han et al., 2020; MacDonald et al., 2022). Due to its importance, OOD detection has received a lot of attention from both industry and academia.

While extensive studies have focused on single-modal OOD detection (Zadorozhny et al., 2022; Roy et al., 2022; Narayanaswamy et al., 2023), multi-modal OOD detection remains underexplored. In reality, multi-modal OOD detection is particularly important to many high-stakes applications like clinical diagnosis and autonomous driving. These applications often fuse information from different data sources and modalities to improve the reliability of decision making. For instance, a majority of AI diagnosis systems integrate multi-modal data, such as radiology imaging (X-ray, ultrasound, CT, MRI, etc.), physician's annotations, and electronic health records, to enhance their prediction performance. In the real-world applications, those multi-modal ML systems inevitably encounter "outlier" conditions caused by various factors, such as machine defects, sensor faults, and operator errors. Hence, a few recent works (Ming et al., 2022b; Esmaeilpour et al., 2022) have explored multi-modal visual-language OOD detection, but they narrow their scope to a special scenario where images come from a new domain. Moreover, these work often employ CLIP-based techniques (Ming et al., 2022a; Miyai et al., 2023; Tao et al., 2023; Miyai et al., 2024) to identify whether a query image matches one of the training set's *class-level labels* (e.g., pneumonia). As a result, these methods fail to identify OOD scenarios such as misaligned pairings of an image and its *fine-grained textual description.*

(a) Misaligned - an ID image not aligned with its textual description (e.g., the textual description belongs to another class).

(b) New-domain - an aligned image-text pair from a dataset of another domain (e.g., containing two birds instead of one).

(c) Noisy - an ID and aligned image-caption pair but with blurry patches (highlighted in red squares) in the image (sensory faults).
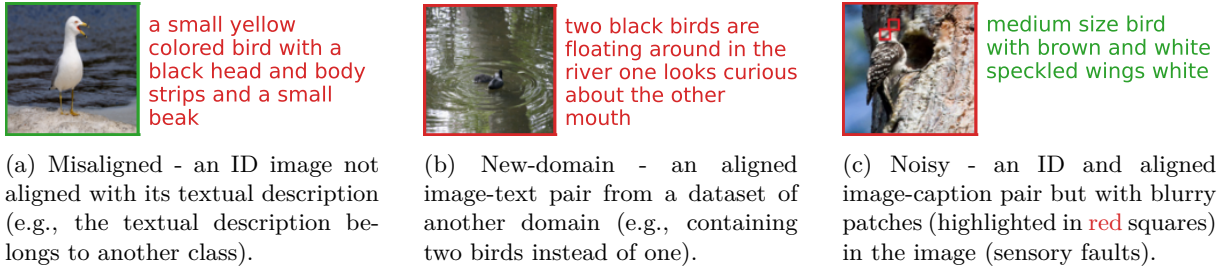
Figure 1: Examples of three OOD scenarios in CUB-200 dataset, with the textual descriptions for each scenario. Images are indicated as OOD with red border, and ID with green. Regarding the text modality, corresponding textual descriptions are in red for OODs and green for IDs.

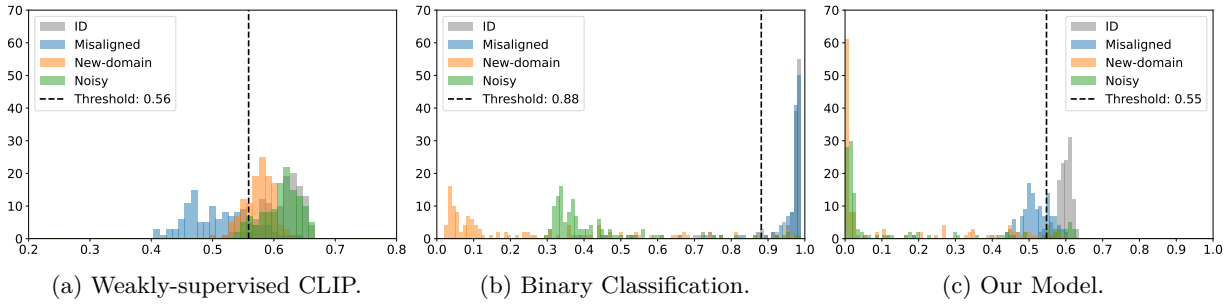(a) Weakly-supervised CLIP. (b) Binary Classification. (c) Our Model.

Figure 2: A motivating example of multi-modal OOD detection on CUB-200 dataset. Following prior work (Ming et al., 2022b), we choose a threshold that includes 95% of in-distribution test samples (gray), and identify a test sample as OOD if its prediction score is *below that threshold*, i.e., to the left of the dashed line. If an OOD detector works effectively, the prediction scores for all samples in all three OOD scenarios should be concentrated to the left of the dashed line. We can observe from (a) that weakly-supervised contrastive learning can only detect *misaligned* OOD samples (blue), but fails to detect *new-domain* and *noisy* OODs. Conversely, a binary classifier in (b) can identify OOD samples in *new-domain* (orange) and *noisy* (green) scenarios, but it does not work for *misaligned* test samples. Motivated by these observations, we develop a general-purpose OOD detection model (c) that can effectively detect OOD samples from all three scenarios.

The goal of this work is to develop a general-purpose multi-modal OOD detection model that can identify OOD in various scenarios in a fine-grained manner. We focus on three different OOD scenarios for multi-sensory data, as illustrated in Fig 1: (1) *Misaligned* - unaligned pairs of data samples, e.g., an in-distribution (ID) image is not aligned with its textual information; (2) *New-domain* - aligned pairs of data samples collected from a new domain, e.g., aligned images and text from a new environment with a different distribution from training; (3) *Noisy* - partially noisy data samples, e.g., images coming from the same environment but with blurry patches. The research question is: How can we detect OOD samples from all these OOD scenarios simultaneously? Existing OOD detection approaches, such as the CLIP-based methods (Ming et al., 2022a; Esmaeilpour et al., 2022; Fort et al., 2021) and weakly-supervised classifications (Ji et al., 2020; Wang et al., 2021), only focus on one of these scenarios (*new-domain* or *noisy*), thus failing to generalize to all of them. Fig. 2 illustrates a motivating example of multi-modal OOD detection on CUB-200 dataset (Wah et al., 2011) using our weakly-supervised CLIP-based contrastive learning method and the binary classifier. We can observe from Fig. 2 (a) that weakly-supervised CLIP can only detect *misaligned* OODs, but is not effective in *new-domain* or *noisy* scenarios. Specifically, weakly-supervised CLIP is not effective for *new-domain* OODs because we deliberately create a more difficult *new-domain* scenario by choosing OODs as samples labeled with "bird" from COCO data (Lin et al., 2014), which has *the same label but different textual information* as those ID samples in the training set of CUB-200, instead of samples with other classes (e.g., person, dog, etc.) in previous works (Ming et al., 2022a; Zhou et al., 2022a; Miyai et al., 2023). In contrast, a binary classifier can only identify *new-domain* or *noisy* OOD samples, but fails in the *misaligned* scenario, as illustrated in Fig. 2 (b). This observation motivates us to develop a new OOD detection model that combines both approaches to complement each other.

Our Contributions. We propose the WOOD, a weakly-supervised multi-modal OOD detection model that can identify three OOD scenarios at the same time. As illustrated in Fig. 3, the proposed WOOD is composed of two components: a binary classifier for classifying OOD samples and a contrastive learning module for measuring the similarity scores between multiple data modalities. On the contrastive learning side, we adopt the Hinge loss to maximize the similarity scores of ID samples and minimize those of OOD samples to better distinguish them. On the binary classifier side, we develop a novel Feature Sparsity Regularizer to better integrate important features from data of multiple modalities. Then a new scoring metric is designed to fuse the prediction results from these two components. Finally, we evaluate the proposed WOOD model on three real-world benchmark datasets. Experimental results demonstrate that our method can successfully identify OOD samples with a high accuracy under three different scenarios, which significantly outperforms the CLIP-based baselines.

2 Related Work

In this section, we review and contrast related work on OOD detection in machine learning. We group them into two categories: single-modal OOD detection and multi-modal OOD detection.

Single-Modal OOD Detection. There exists a plethora of works on single-modal OOD detection (Salehi et al., 2022) for machine learning. They can be generally categorized into three types: (i) vision OOD detection, (ii) text OOD detection, and (iii) time-series OOD detection (Du et al., 2022). For vision OOD detection, various methods have been developed, including softmax confidence score (DeVries & Taylor, 2018; Hein et al., 2019; Hendrycks & Gimpel, 2017; Huang & Li, 2021), energy-based score (Yang et al., 2021; Sun et al., 2021; Sun & Li, 2022), distance-based method (Sun et al., 2022; Ren et al., 2021; Podolskiy et al., 2021; Techapanurak et al., 2020; Zaeemzadeh et al., 2021; Van Amersfoort et al., 2020), and generative models (Li et al., 2022b; Xiao et al., 2020). For instance, Liu et al. (2020) proposed an energy-based OOD detection method with theoretical analysis. Sun et al. (2022) developed nearest neighbors to improve the flexibility and generality of OOD detection. For text OOD detection, pre-trained language models (Podolskiy et al., 2021; Zhou et al., 2021) are commonly used due to their robustness in identifying OOD samples in natural languages. Other methods, such as data augmentation (Zhan et al., 2021) and contrastive learning (Zhou et al., 2022b; 2021), have also been developed for OOD detection. Furthermore, some researchers have focused on OOD detection in time-series data (Romero & Estévez, 2022; Kaur et al., 2022; Georgescu et al., 2021), where several ML models have been developed for video anomaly detection (Georgescu et al., 2021; Wang et al., 2018). Wang et al. (2018) combined LSTM with CNN to improve anomaly detection using a spatio-temporal auto-encoder. Li et al. (2022a) leveraged generative models to predict middle frames based on past and future frames. However, these methods mainly detect OOD samples using unimodal data, such as images or text. In contrast, we develop a general-purpose model that combines multi-modal data, such as images and textual information, to enhance the performance of OOD detection.

Multi-Modal OOD Detection. Some studies (Sun et al., 2020; Wang et al., 2021) have adopted multi-modal data to improve the OOD detection accuracy based on deep neural networks (DNNs). (Wang et al., 2021) proposed a multi-modal transformer network that combines Radar and LiDAR data to detect radar ghost targets. Ji et al. (2020) developed a supervised VAE (SVAE) model that integrates sensor data of multiple modalities to detect an anomalous operation mode of the car. To improve the accuracy of detecting abnormal driving segments, Qiu et al. (2022) developed an unsupervised contrastive approach that uses generative adversarial networks to extract latent features from five modalities. More recently, CLIP-based methods (Ming et al., 2022a; Esmaeilpour et al., 2022; Fort et al., 2021) have been developed to detect OOD samples. (Esmaeilpour et al., 2022) designed a zero-shot OOD detection model based on pre-trained CLIP (Radford et al., 2021) to detect and generate candidate labels for test images of unknown classes. However, this method heavily relies on a set of candidate labels. To overcome this issue, Ming et al. (2022a) developed a zero-shot method called Maximum Concept Matching (MCM) based on a pre-train CLIP model, that can detect visual OOD samples, i.e., OODs arising from the image modality. Miyai et al. (2023) further introduced Global-Local(GL)-MCM, which utilizes local CLIP visual features to enable zero-shot OOD detection for background-related OOD features. Furthermore, latest research explored various fine-tuning strategies for CLIP, such as prompt learning (Zhou et al., 2022a; Miyai et al., 2024) and outlier synthesis (Tao et al., 2023), for enhanced OOD detection based on MCM and GL-MCM. While these methods have shown

good performance on multi-modal OOD detection, they can only detect visual OOD samples rather than both an image and its associated textual description. Hence, they are not applicable to other OOD scenarios we are exploring, such as misalignment and noisy examples.

Different from prior works, we develop a general-purpose multi-modal OOD detector that can identify OOD samples arising from three different scenarios in a fine-grained manner. Our proposed method leverages both weakly supervised learning and contrastive learning for improving OOD detection.

3 Preliminaries

This section begins by introducing the problem of detecting OOD samples in multi-modal data. Subsequently, we delve into the applications of contrastive learning for multi-modal OOD detection

3.1 Problem Statement

We consider the problem of detecting multi-modal OOD samples under three different scenarios, as mentioned in Sec. 1. In this paper, we use vision-language modeling as a running problem for multi-modal OOD detection. Given a batch of N pairs of images and texts, along with their positive ID labels, denoted by $\{(x_n, t_n), y_n = 1\}_{n=1}^N$, we generate a small number of OOD samples K during training. Specifically, we randomly select $K \ll N$ pairs of images and texts and convert them to OODs according to the three scenarios above, such that $\{(x_k, t_k), y_k = 0 | k \in \{k_1, \ldots, k_K\} \subset \{1, \ldots, N\}\}$, and the remaining $N - K$ ID pairs are unchanged. The goal of this work is to improve the OOD detection performance for multiple scenarios using weak supervision on a small number of generated OOD samples.

3.2 Contrastive Learning

Contrastive learning aims to encode pairs of data samples into latent representations by making similar samples close to each other and dissimilar ones far apart. One well-known method is the vision-language pre-trained model CLIP, which jointly trains an image encoder and a text encoder to learn the latent representations from text paired with images using zero-shot learning. Specifically, it encodes a pair of image x_n and text t_n into the latent representations $\mathcal{I}(x_n)$ and $\mathcal{T}(t_n)$, respectively, and then adopts cosine similarity to minimize the distance of their representations $\mathcal{I}(x_n)$ and $\mathcal{T}(t_n)$. Due to its excellent performance in learning the latent representations of images and texts, a few CLIP-based methods have been developed to detect multi-modal OOD samples. However, existing methods can only detect one specific scenario where a given image and its textual information come from a new domain with a distribution shift. In the following section, we develop a general-purpose OOD detection framework to identify OODs arising from several different scenarios.

4 Proposed Model

In this section, we describe the proposed multi-modal OOD detection framework and then devise a new scoring metric for detecting OODs under three different scenarios.

We propose a weakly-supervised OOD detector, called WOOD, that combines a classifier and contrastive learning to simultaneously detect three different OOD scenarios mentioned in Section 1. Fig. 3 illustrates the overall multi-modal OOD detection framework that consists of two components: a contrastive learning module and a binary classifier. The core idea is to use contrastive learning to learn the representations of different data modalities by enforcing the similarity scores of ID pairs to be higher than those of OOD samples. Then WOOD combines the similarity scores from contrastive learning and the prediction results from a binary classifier to identify OOD samples. Below, we detail the two main components of the proposed WOOD method.

Contrastive Learning with Hinge Loss. Inspired by CLIP-based OOD detection methods, we adopt an image encoder and a text encoder to learn the representations of input pairs (image and text) using
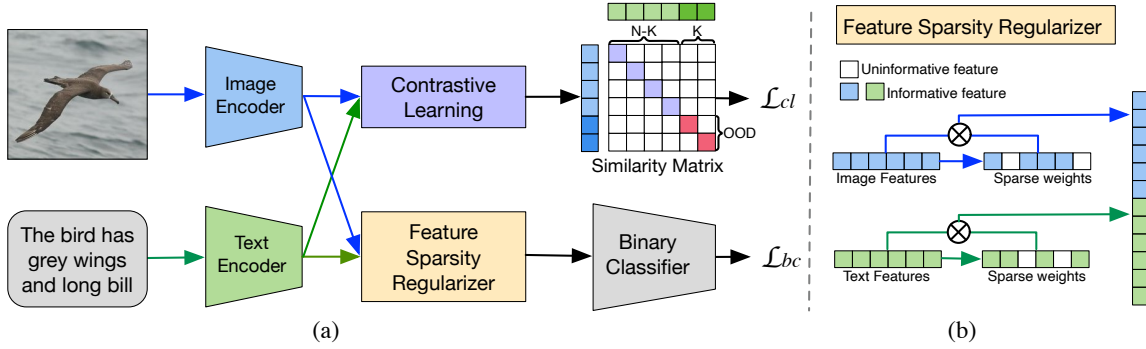
Figure 3: (a) The overall framework of the WOOD detector. It consists of two main parts: 1) a constrastive learning module and 2) a binary classifier. Contrastive learning aims to maximize the difference in similarity scores between ID and OOD samples while the binary classifier is used to predict the probability of being OOD. (b) An expanded detailed view of the Feature Sparsity Regularizer in the WOOD framework. This regularizer integrates important features from data of multiple modalities to improve classification accuracy.

contrastive learning. However, unlike existing zero-shot CLIP-based detectors, we add a small number of OOD samples to better separate the representations of ID and OOD samples. Thus, our goal is to maximize the cosine similarity of representations learned from ID samples but and minimize those of OOD samples. Let (x_n, t_n) be a pair of input image and text, and their corresponding representations denote $(\mathcal{I}(x_n), \mathcal{T}(t_n))$. Then, the CLIP contrastive loss (Radford et al., 2021) can be modified to maximize the *cross entropy* of the cosine similarity between labeled OOD pairs and minimize that of ID pairs, which is given by:

$$\mathcal{L}_1 = -\frac{1}{N-K} \sum_{n=1}^{N-K} \log \frac{e^{S_{id}(x_n^+, t_n^+)}}{\sum_{i=1}^{N-K} e^{S_{id}(x_n^+, t_i^+)}} + \frac{1}{K} \sum_{k=1}^{K} \log \frac{e^{S_{ood}(x_k^-, t_k^-)}}{\sum_{i=1}^{K} e^{S_{ood}(x_k^-, t_i^-)}}, \quad (1)$$

where $S_{id}(x_n^+, t_n^+) = \frac{\mathcal{I}(x_n^+) \cdot \mathcal{T}(t_n^+)}{\|\mathcal{I}(x_n^+)\|\|\mathcal{I}(t_n^+)\|}$ and $S_{ood}(x_k^-, t_k^-) = \frac{\mathcal{I}(x_k^-) \cdot \mathcal{T}(t_k^-)}{\|\mathcal{I}(x_k^-)\|\|\mathcal{I}(t_k^-)\|}$ represent the cosine similarity between image and text features for ID and OOD pairs, respectively. Here "+" and "-" mean the sample is from ID and OOD, respectively. In addition, $N-K$ and K respectively denote the number of ID and OOD pairs.

To further maximize the difference in latent representations between ID and OOD samples, we adopt Hinge loss instead of $\mathcal{L}_1$ in Eq. 1 to constrain their cosine similarity. In this work, we consider Hinge loss for both ID pairs and labeled OOD pairs in the objective function.

First, we introduce Hinge loss for $N-K$ ID samples, as shown in the upper part of the similarity matrix in Fig 3. It is given by:

$$\mathcal{L}_{id} = \sum_{n=1}^{N-K} \left(\frac{1}{N} \sum_{i=1, i\neq n}^{N} \max\left(0, m - S_{id}(x_n^+, t_n^+) + S_{id}(x_n^+, t_i^{+/-})\right) \right), \quad (2)$$

where m is a margin, $S_{id}(x_n^+, t_n^+)$ represents the cosine similarity of $N-K$ aligned ID pairs and $S_{id}(x_n^+, t_i^{+/-})$ represents the cosine similarity between $N-K$ ID images and all N texts (including OOD samples), where each text either does not align with its corresponding ID image or belongs to an OOD sample. In short, the objective, $\mathcal{L}_{id}$, aims to maximize the difference between the aligned ID pairs and incorrect pairings by ensuring that such difference is larger than a margin m.

Second, we introduce Hinge loss for K OOD samples to constrain their cosine similarity to a small value. Hence, we have:

$$\mathcal{L}_{ood} = \sum_{k=1}^{K} \left(\frac{1}{N} \sum_{i=1}^{N} \max\left(0, -m + S_{ood}(x_k^-, t_i^{+/-})\right) \right), \quad (3)$$

where $S_{ood}(x_k^-, t_i^{+/-})$ represents the cosine similarity between each of K OOD images and all N texts (including OOD samples). By definition, the K OOD images should not align with any of the $N-K$ ID texts, since each OOD image is not aligned with its corresponding text as described in the *misaligned*

scenario. Additionally, we should discourage the model from aligning *new-domain* and *noisy* OOD image-text pairs.

By combining the above loss functions, $\mathcal{L}_{id}$ and $\mathcal{L}_{ood}$, for ID and OOD samples, the overall contrastive loss is given by:

$$\mathcal{L}_{cl} = \frac{1}{N}\left(\mathcal{L}_{id} + \mathcal{L}_{ood}\right). \tag{4}$$

During inference, inspired by Wang et al. (2023a), we apply the sigmoid function σ to the cosine similarity to obtain the OOD predictions:

$$P_{cl} = \sigma(S(x_n, t_n)), \tag{5}$$

where $S(x_n, t_n)$ denotes the cosine similarity.

Binary Classifier. We further adopt weakly-supervised learning to classify OOD samples since recent studies have illustrated that it can significantly outperform unsupervised learning methods by adding some OOD samples (Tian et al., 2020; Sultani et al., 2018; Majhi et al., 2021). However, the challenge lies in how to integrate image and text features for improved classification accuracy. One naive method is to concatenate their embeddings directly and then feed them into a classifier. But this simple fusion approach does not perform well since the informativeness of different features may vary for different samples (Jiang et al., 2023; Han et al., 2022). To address this issue, we develop a new feature sparsity regularizer to select and integrate important features from data of the two modalities, as illustrated in Fig. 3(b). Specifically, we train encoder networks $E^{\mathcal{I}} : \mathcal{I}(x_n) \to w_n^{\mathcal{I}}$ and $E^{\mathcal{T}} : \mathcal{T}(t_n) \to w_n^{\mathcal{T}}$ to use features obtained from image encoder and text encoders, These features are updated by a sigmoid activation σ to assign higher weights to informative features and lower weights to the uninformative features. Namely, the weight vectors $\sigma(w_n^{\mathcal{I}})$ and $\sigma(w_n^{\mathcal{T}})$ are multiplied with $\mathcal{I}(x_n)$ and $\mathcal{T}(t_n)$ respectively. After that, we fuse the features from two modalities by concatenation, yielding $h_n = \oplus[\mathcal{I}(x_n) \otimes \sigma(w_n^{\mathcal{I}}), \mathcal{T}(t_n) \otimes \sigma(w_n^{\mathcal{T}})]$. Next, we adopt a binary classifier to identify ID/OOD samples based on the fused features h_n. To introduce sparsity in the weight vectors, we use L_1 normalization $\|\sigma(w_n^{\mathcal{I}})\|_1$ and $\|\sigma(w_n^{\mathcal{T}})\|_1$ and add them to our binary cross entropy (BCE) loss function, which is given by:

$$\mathcal{L}_{bc} = \frac{1}{N}\left(\sum_{i=1}^{N} \text{BCE}(y_i, \hat{y}_i) + \|\sigma(w_n^{\mathcal{I}})\|_1 + \|\sigma(w_n^{\mathcal{T}})\|_1\right) \tag{6}$$

where $\text{BCE}(y_i, \hat{y}_i) = -\left(y_i \log(\hat{y}_i) + (1 - y_i)\log(1 - \hat{y}_i)\right)$. Note that here $y_i = 0$ means the i-th test sample is OOD while it is an ID sample when $y_i = 1$.

Overall objective. Finally, we jointly train the contrastive learning module and binary classifier for OOD detection. The overall objective for multi-OOD detection is given by

$$\mathcal{L} = (1 - \lambda)\mathcal{L}_{cl} + \lambda\mathcal{L}_{bc}, \tag{7}$$

where $\mathcal{L}_{bc}$ is the contrastive loss, $\mathcal{L}_{bc}$ is the binary cross-entropy loss for the classifier, and λ is the weight for balancing the two respective terms.

4.1 New Scoring Metric

To improve the performance of OOD detection during inference, we introduce a novel scoring metric that combines predictions from the contrastive learning module and the binary classifier. The key insight is that we identify an image and text pair as ID only when both the contrastive learning and binary classifier predict that sample as ID. In all other cases, we identify it as OOD. We codify this condition with the following scoring metric for identifying OOD samples:

$$P_{ood} = 1 - P_{bc}P_{cl}, \tag{8}$$

where P_{bc} and P_{cl} denote the prediction results from the binary classifier and contrastive learning, respectively. Subsequent sections demonstrate that the new scoring metric can help detect OOD samples in all three OOD scenarios effectively.

4.2 Summary of Proposed Model

We summarize the proposed WOOD model in Algorithm 1. The basic idea is to map ID and OOD pairs (image and text) into latent representations, and then calculate their cosine similarity. Then, we use Hinge loss to maximize the difference in similarity scores between ID and OOD samples. Moreover, we feed the fused latent representations into a binary classifier to classify ID or OOD samples. Finally, we jointly train the binary classifier and the contrastive learning component for OOD detection.

Algorithm 1 The Proposed WOOD Model

1: **Input:** A batch of N pairs of images and texts, with $N - K$ ID pairs and K labeled OOD pairs.
2: **Output:** Samples labeled as OOD or ID.
3: Encode ID pairs into $\mathcal{I}(x_n^+)$ and $\mathcal{T}(t_n^+)$.
4: Encode OOD pairs into $\mathcal{I}(x_n^-)$ and $\mathcal{T}(t_n^-)$.
5: Compute Hinge loss on cosine similarity for ID samples according to Eq. 2 and OOD samples according to Eq. 3 for contrastive learning.
6: Compute the total contrastive loss $\mathcal{L}_{cl}$ in Eq. 4.
7: Compute loss of the binary classifier $\mathcal{L}_{bc}$ in Eq. 6.
8: Jointly train the binary classifier and contrastive learning based on the overall objective in Eq. 7.
9: Identify OOD samples based on the designed scoring metric in Eq. 8.

---

5 Experiments

In this section, we carry out extensive experimentation to evaluate the performance of the proposed WOOD model on multiple benchmark datasets. Then, we conduct ablation studies to explore how the main components in model design and hyperparameters impact OOD detection performance.

5.1 Datasets

We implement experiments on the three real-world datasets: CUB-200 (Wah et al., 2011), MIMIC-CXR (Johnson et al., 2019), and COCO (Lin et al., 2014). For CUB-200, the textual information comes from literature (Reed et al., 2016). COCO and MIMIC-CXR contain images and their corresponding textual descriptions.

Three OOD scenarios. We generate three different OOD scenarios using the above datasets as follows.

- **Misaligned**. Randomly select a subset of ID images and their textual description from a given dataset and shuffle them so that each image is not aligned with its corresponding textual information. Specifically, select images from one category and the unaligned textual descriptions from another category, ensuring that each pair of OOD images and text are not aligned.
- **New-domain**. Choose OOD samples from another new dataset different from the training data. For instance, when conducting experiments on MIMIC-CXR data, select some pairs of texts and images from Indiana University (IU) X-ray (Demner-Fushman et al., 2016) as OOD samples.
- **Noisy**. Add Gaussian blur (whitening for X-ray images) to several patches in the ID images, such that each image is partially blurry but its corresponding textual information is correct.

Table 1 summarizes the detailed information about generating three OOD scenarios using the above datasets in the experiments.

Table 1: Detailed Summary of Our Three OOD Scenarios.

Scenarios	CUB-200	MIMIC-CXR	COCO
Misaligned	Randomly select pairs of ID images and texts, swap their textual descriptions with textual descriptions of images from different categories, and label these misaligned pairs as OOD.		
New-domain	Samples from COCO with birds	IU X-ray (Demner-Fushman et al., 2016)	GCC (Sharma et al., 2018)
Noisy	Randomly select pairs of ID images and texts, add a small number of blurry/whitened patches to each, and label these blurry pairs as OOD.		

5.2 Model Configurations

Following prior CLIP-based detectors, we also use the CLIP model (ViT-B/16 (Radford et al., 2021)) as the backbone of the contrastive learning module. The two encoders are $CLIP_{image}$ and $CLIP_{text}$, which are pre-trained Transformer models for image and text (Radford et al., 2021) respectively. We do not change the base encoders but fine-tune them with Hinge loss in Eq. (4) for both feature alignment and OOD detection. Recall that WOOD also has a Feature Sparsity Regularizer module (Figure 3), which is a single projection layer (MLP) with a sigmoid activation. We set its hidden size to 512, the same as the dimensions of the output embeddings from $CLIP_{image}$ and $CLIP_{text}$. The Binary Classifier is a 3-layer fully connected network with ReLU activation, which outputs a single probability score for binary OOD classification and the layer hidden size is 1024, 512, and 128 respectively. We train the proposed WOOD model using Adam optimizer (Kingma & Ba, 2014) with initial learning rate $5e^{-6}$ and stepped learning rate schedule. Additionally, the batch size is set to 128 in all experiments, and $\lambda = 0.8$ for the overall training adjective in Eq. (7). Regarding the margin of the Hinge loss, we choose $m = 0.2$ for CUB-200 and MIMIC-CXR, and $m = 0.3$ for COCO after grid search. Note that subsequent ablation studies in Section 5.5 explore the impact of these hyper-parameters on detection performance. To improve detection performance on three scenarios simultaneously, we randomly select 1% of the training data and replace them with labeled OOD samples for each scenario during training, as described in Tab. 1, resulting in a total of 3% OOD samples and 97% of ID samples for weakly-supervised training. During evaluation, we use the same ratio (25%) of test samples for ID and three OOD scenarios. Finally, regarding inference, following previous research (Ming et al., 2022b), we choose a threshold δ (e.g., 0.6) at inference so that a high fraction of ID data is above the threshold (i.e., OOD samples are identified when $P_{ood} > 1 - \delta$). Following prior work (Ming et al., 2022b), we report the false positive rate for 95% of recall of ID samples, FPR95, to measure the prediction error when OODs are identified by threshold δ. Additionally, we report the AUROC scores, which is a threshold-free OOD detection metric commonly used in the literature (Hendrycks & Gimpel, 2016; Liu et al., 2020; Ming et al., 2022a).

5.3 Baselines

We compare the WOOD model against a broad range of CLIP-based OOD detection baselines, including zero-shot (1-2) and finetuned approaches (3-6), as well as the weakly-supervised implementation (7-8) of previous detection methods based on auxiliary OOD data.

1. **MCM-OOD** (Ming et al., 2022a). This method uses zero-shot CLIP for multi-modal OOD detection based on Maximum Concept Matching (MCM). It can only detect visual OODs, i.e. OOD images, in one type of scenario in which a given image is not aligned with its label in the training data.
2. **GL-MCM-OOD** (Miyai et al., 2023). As an extension of MCM-OOD, this work leverages both local and global visual-text alignments of CLIP features, known as Global-Local MCM (GL-MCM), to detect OOD samples containing ID classes with OOD features in the background in the zero-shot manner. However, it still only detects visual OODs.
3. **CoOp-MCM** (Miyai et al., 2023). This method adopts prompt learning to finetune the pre-trained CLIP using a set of learnable context vectors (Context Optimization). In addition, it uses MCM scores to detect visual OODs.
4. **NPOS-MCM** (Tao et al., 2023). This method finetunes the pretrained CLIP for enhanced OOD detection by generating artificial outliers from the boundary ID training data selected based on the non-parametric k-nearest-neighbor (k-NN) distance. It also utilizes MCM scores to detect visual OODs.
5. **CLIP-N** (Wang et al., 2023b). This model adopts a learnable "no" text encoder in addition to the pre-trained CLIP to capture negation semantics. It also uses a threshold-free inference algorithm to perform OOD detection by utilizing the association between negation semantics from "no" prompts and the image encoder.
6. **LoCoOp** (Miyai et al., 2024). This work extends CoOp by performing OOD regularization that utilizes the CLIP local features as OOD features during training, since local features tend to have OOD related nuances such as background objects. It adopts GL-MCM scores to detect visual OODs.

Table 2: Performance comparison of different methods for OOD detection on CUB-200 dataset averaged over three random seeds. Higher AUROC and lower FPR95 indicate better performance.

Methods	Misaligned+ID		New-domain+ID		Noisy+ID		All Scenarios+ID	
	AUROC↑	FPR95↓	AUROC↑	FPR95↓	AUROC↑	FPR95↓	AUROC↑	FPR95↓
Zero-shot								
MCM-OOD	47.16	94.76	81.42	62.72	51.62	93.82	60.07	90.52
GL-MCM-OOD	46.90	96.33	79.88	72.50	49.60	96.25	58.80	94.42
Finetuned								
CoOp-MCM	48.61	95.76	90.30	48.83	52.83	95.55	63.91	94.11
NPOS-MCM	49.46	94.58	52.34	92.67	46.71	93.83	49.50	94.08
CLIP-N	49.96	96.00	80.21	83.33	49.64	95.17	59.94	95.17
LoCoOp	49.25	95.92	91.72	42.58	54.20	92.92	65.05	91.90
Weakly-supervised								
CLIP-Energy	49.45	95.25	78.51	83.50	50.08	95.67	59.35	93.58
CLIP-BCE	50.37	94.83	88.61	29.50	95.10	15.67	78.08	46.87
Ours	**90.66**	**32.75**	**99.38**	**2.83**	**95.57**	**10.92**	**95.20**	**15.50**

Table 3: Performance comparison of different methods for OOD detection on MIMIC-CXR dataset averaged over three random seeds. Higher AUROC and lower FPR95 indicate better performance.

Methods	Misaligned+ID		New-domain+ID		Noisy+ID		All Scenarios+ID	
	AUROC↑	FPR95↓	AUROC↑	FPR95↓	AUROC↑	FPR95↓	AUROC↑	FPR95↓
Zero-shot								
MCM-OOD	53.43	96.89	50.92	93.54	47.19	96.01	50.49	95.55
GL-MCM-OOD	54.15	95.54	57.05	90.05	47.15	96.29	52.78	94.41
Finetuned								
CoOp-MCM	33.41	97.90	66.82	69.46	50.76	94.80	53.00	95.27
NPOS-MCM	47.83	94.90	57.81	88.64	52.22	94.94	52.62	93.19
CLIP-N	64.21	88.58	50.69	86.56	50.93	95.16	55.28	91.24
LoCoOp	33.73	97.34	62.27	68.44	51.11	94.12	49.04	94.89
Weakly-supervised								
CLIP-Energy	64.71	89.80	93.32	54.51	50.05	94.12	69.33	89.94
CLIP-BCE	56.52	93.24	99.87	0.59	82.44	39.03	79.45	42.70
Ours	**87.46**	**43.28**	**99.95**	**0.22**	**97.22**	**6.80**	**94.87**	**16.78**

7. **CLIP-Energy** (Liu et al., 2020). This approach adopts auxiliary OOD data to finetune the CLIP model using energy scores. For a fair comparison, we utilize the same number of OOD samples as our method for energy finetuning.

8. **CLIP-BCE** (Liznerski et al., 2022). This model finetunes the pre-trained CLIP with a binary classifier (BCE) in the supervised manner using our OOD samples as outliers for Outlier Exposure (Hendrycks et al., 2018), which aims to maximize the similarity of an image and the ID label set and minimize that for OOD samples.

5.4 Main Results

We conduct extensive experiments to thoroughly evaluate the detection performance of WOOD using three benchmark datasets. Here, recall that the proposed WOOD is weakly-supervised on training datasets containing 97% ID samples and 1% generated OOD samples for each of the three scenarios. To create a balanced evaluation setting, the test datasets are equally distributed for ID and our three OOD scenarios (25% each). We report the results on three subsets of the test dataset for each scenario (i.e. Misaligned+ID, New-domain+ID, and Noisy+ID), as well as the overall performance on the entire test set.

We first assess the performance of the proposed WOOD on CUB-200 dataset. Table 2 illustrates the comparison results of different OOD detection methods using three random seeds. We can observe from this table that our method is effective in all three OOD scenarios, and its overall performance significantly exceeds the

Table 4: Performance comparison of different methods for OOD detection on COCO dataset averaged over three random seeds. Higher AUROC and lower FPR95 indicate better performance.

Methods	Misaligned+ID		New-domain+ID		Noisy+ID		All Scenarios+ID	
	AUROC↑	FPR95↓	AUROC↑	FPR95↓	AUROC↑	FPR95↓	AUROC↑	FPR95↓
Zero-shot								
MCM-OOD	40.86	97.99	71.15	68.05	47.39	96.15	53.13	95.42
GL-MCM-OOD	35.44	99.73	86.29	46.40	47.66	96.53	56.50	98.40
Finetuned								
CoOp-MCM	56.31	95.50	68.21	72.16	44.51	96.13	56.34	93.45
NPOS-MCM	34.06	96.04	74.81	92.57	49.32	95.98	52.73	95.57
CLIP-N	61.97	85.24	72.73	78.61	55.33	92.14	63.35	87.91
LoCoOp	55.11	94.68	89.56	43.77	43.74	96.10	62.80	93.75
Weakly-supervised								
CLIP-Energy	57.83	84.73	96.07	24.46	52.65	93.84	68.85	86.88
CLIP-BCE	56.95	93.56	98.39	6.69	98.73	6.09	84.69	35.47
Ours	**99.78**	**1.14**	**99.88**	**0.88**	**99.08**	**2.89**	**99.58**	**1.54**

baselines. The main reason is that our method leverages both contrastive learning and a binary classifier for OOD detection on all three scenarios, as motivated by Fig. 2. Evidently, zero-shot methods such as MCM-OOD and GL-MCM-OOD do not perform well since they are only designed for detecting visual OODs by querying an image to check whether the returned features from CLIP align with training labels. In addition, although finetuned CLIP methods are designed to improve the detection performance on *new-domain* OODs, we discover that finetuning approaches such as NPOS-MCM and CLIP-N can have an adverse effect on performance when when there are not many OOD training images from classes distinguishable from "bird". In particular, when NPOS-MCM generates training OOD examples on the k-NN boundary of ID images, these examples can overlap with ID images from another classes instead of OODs from COCO-bird, resulting in worse performance than zero-shot methods. Also, while CLIP-N can embed negation semantics from images to "no" text prompts, these semantics may not be sufficiently distinct from ID "bird" features. On the other hand, CoOp and LoCoOp effectively build contexts from CLIP image features around the associated class labels, resulting in better *new-domain* detection. Despite taking advantage of OOD training data, the small number of training OODs is not sufficient for CLIP-Energy and CLIP-BCE to beat context prompt fine-tuning for *new-domain* examples. Similarly to our method, CLIP-BCE can utilize weakly-supervised binary classification to effectively detect *noisy* visual OOD examples, but it still fails to detect *misaligned* textual OODs. In contrast, our method can detect both visual and textual OODs. Still, it is very challenging to identify a pair of OOD samples when an image is slightly unaligned with its textual information. Specifically in our experiment, *misaligned* test samples include many similar images as those in the ID samples, while the textual descriptions also contain "bird" with hardly different fine-grained features. As a result, the FPR95 score for detecting *misaligned* OODs is higher compared to other scenarios.

Next, we also show that WOOD can identify OOD samples in multi-modal medical data, MIMIC-CXR. As illustrated in Table 3, it can be observed that the proposed method effectively detects OODs in all three OOD scenarios and its overall performance is better than the baselines. Here, note that similar to CUB-200, the FPR95 of the *misaligned* scenario is also high since the test images have the same class label "chest scans" as those in the training data and only have *slightly different textual descriptions*. Furthermore, zero-shot and finetuned CLIP methods fail to detect OODs in all three scenarios because the pre-trained CLIP lacks the alignment capability for the medical image features and data labels, which is absent from its pretraining data. With additional weakly-supervised training, CLIP-Energy and CLIP-BCE can learn better energy-based OOD scores or binary predictions respectively to significantly improve the detection performance for *new-domain* samples. However, CLIP-BCE falls short in detecting *noisy* OOD samples in this experiment with higher false positives. One possible explanation is that while a classifier is effective at detecting visual noise, the binary classifier in CLIP-BCE aligns the image features with the collection of ID class labels, instead of the corresponding textual descriptions using contrastive learning. On the other hand, this issue is clearly mitigated by the interplay of our two components where our proposed method first aligns medical images with their detailed textual description with constrastive learning, then combines

the learned features in conjunction with feature sparsity to make accurate predictions for all three OOD scenarios simultaneously.

Furthermore, we apply the proposed WOOD to detect OOD samples on COCO dataset. We compare the detection performance of different methods as shown in Table 4. It can be seen that our approach is able to effectively detect OODs in all three OOD scenarios while the baseline methods can only detect *new-domain* or *noisy* OODs. In addition, since COCO and its corresponding *new-domain* dataset GCC both mostly contain images with the class label "person", zero-shot and finetuned CLIP baselines with except GL-MCM-OOD and LoCoOp struggle to detect these OODs. The reason why GL-MCM-OOD and LoCoOp outperform the other baselines is that they can capture local CLIP features representative of OOD in the image background in the learnable context prompts around the class labels, as previously demonstrated by Miyai et al. (2023) and Miyai et al. (2024). However, by utilizing a small number of OOD training data, weakly-supervised classification methods such as CLIP-BCE and ours can capture these OOD nuances even more effectively, as evidenced by their superior performance for detecting *new-domain* OODs, as well as *noisy* visual OOD examples. Moreover, the detection performance for *misaligned* OODs is much higher than the previous two datasets, since COCO has a much larger training set that contains many easily distinguishable classes (e.g. person, cat, bird, etc.).

5.5 Ablation Studies

In this section, we conduct ablation studies to investigate the effect of some important components, the weight in the objective function as well as the Hinge loss and its hyperparameter on the OOD detection performance.

Effect of Main Model Components. First, we investigate the effect of using individual model components against the proposed WOOD model. We can see from Table 5 that if we only use one of two main components, the detection accuracy could drop significantly. It indicates that the binary classifier and contrast learning modules complement each other for enhance the OOD detection performance. More specifically, as observed in Fig. 2, it can be seen that for the CUB-200 dataset, the contrastive learning module does not effectively detect *new-domain* and *noisy* samples while the binary classifier can separate these OODs from ID samples successfully.

Table 5: Performance comparison between individual model components and our proposed combined method averaged over three random seeds. It can be seen that our proposed method outperforms both the contrastive learning and binary classifier on all three datasets.

Components	Dataset					
	CUB-200		MIMIC-CXR		COCO	
	AU-ROC	FPR95	AU-ROC	FPR95	AU-ROC	FPR-95
Contrastive Learning	75.49	67.64	72.58	68.43	77.22	62.56
Binary Classification	82.07	34.78	72.15	59.13	92.25	22.52
Ours	**95.20**	**15.50**	**94.87**	**16.78**	**99.58**	**1.54**

Effect of Weight in the Objective. We study the effect of the weight in the objective function (λ in Eq. (7)) on the performance of OOD detection. We can see from Table 6 that the proposed WOOD model has the best performance when $\lambda = 0.4$ as λ decreases from 0.5 to 0.2 on all three datasets. Note that when $\lambda = 0.5$, the contrastive learning module and the binary classifier have equal weights in the objective. For more challenging datasets with highly similar images such as CUB-200 and MIMIC-CXR, low λ values have much more pronounced negative impact on the OOD detection performance, as the model becomes less effective in detecting *new-domain* and *noisy* scenarios. This further supports our motivation for combining two different modules in the proposed WOOD.

Effect of Hinge Loss and its Hyperparameter. We also explore the impact of Hinge loss (in Eq. equation 2 and Eq. equation 3) on the detection performance. Table 7 shows the detection performance under different margin parameters. In addition, we ablate the Hinge loss (Eq. 4) to investigate its impact on the model performance. Specifically, the model without the Hinge loss utilize $\mathcal{L}_1$ as defined in Eq. 1 for contrastive learning. We can observe from Table 7 that our method performs the best performance when

Table 6: Impact of the weight of the binary classifier in the objective on detection performance. We report the results averaged over three random seeds. It can be seen that the proposed WOOD performs very well when $\lambda = 0.4$ on all three datasets.

| λ | Dataset | | | | | |
| | CUB-200 | | MIMIC-CXR | | COCO | |
	AU-ROC	FPR95	AU-ROC	FPR95	AU-ROC	FPR-95
0.5	95.19	15.72	94.74	17.20	99.49	1.66
0.4	**95.20**	**15.50**	**94.87**	**16.78**	**99.59**	1.47
0.3	90.55	30.20	94.08	19.33	99.46	**1.20**
0.2	82.57	40.97	85.28	38.11	99.39	1.54

$m = 0.2$ for CUB-200 and MIMIC-CXR. Since COCO has many easily distinguishable classes, our model benefits from using a slightly large margin $m = 0.3$. Moreover, our detection method without the Hinge loss ($\mathcal{L}_1$) does not perform well for CUB-200 and MIMIC-CXR. Therefore, we can conclude that this Hinge loss plays an important role in multi-modal OOD detection.

Table 7: Impact of Hinge loss in the objective on detection performance. We report the averaged results from three random seeds. It can be observed that when $m = 0.2$, the proposed model has the best performance on CUB-200 and MIMIC-CXR datasets. For COCO data, it performs best as $m = 0.3$.

| $\mathcal{L}_{cl}$ | Dataset | | | | | |
| | CUB-200 | | MIMIC-CXR | | COCO | |
	AU-ROC	FPR95	AU-ROC	FPR95	AU-ROC	FPR-95
No Hinge	81.42	41.11	86.90	29.78	99.01	2.09
$m = 0.1$	94.27	18.95	92.74	21.84	99.35	1.87
$m = 0.2$	**95.20**	**15.50**	**94.87**	**16.78**	99.48	1.65
$m = 0.3$	94.68	17.41	93.21	20.75	**99.58**	**1.54**
$m = 0.4$	92.57	25.61	93.77	19.80	99.37	1.87

Effect of the Feature Sparsity Regularizer. Last but not least, we conduct ablations of the Feature Sparsity Regularizer (FSR) used in the binary classifier to measure its usefulness for OOD detection. From Table 8, it can be observed that using sparse features for the binary classifier is beneficial for the detection performance, especially for the medical data. Since the textual description for each image contains about 40 words on average in MIMIC-CXR, the FSR module encourages the binary classifier to gather highly informative features from the text modality for OOD classification.

Table 8: Impact of the Feature Sparsity Regularizer (FSR) used in the binary classifier on detection performance. Averaged results from three random seeds show that employing FSR leads to superior performance across all three datasets.

| FSR | Dataset | | | | | |
| | CUB-200 | | MIMIC-CXR | | COCO | |
	AUROC↑	FPR95↓	AUROC↑	FPR95↓	AUROC↑	FPR95↓
No	94.75	15.64	84.41	37.21	99.23	1.64
Yes	**95.20**	**15.50**	**94.87**	**16.78**	**99.58**	**1.54**

6 Conclusions and Future Work

In this paper, we developed WOOD, a general-purpose multi-modal OOD detection framework that integrates contrastive learning and a binary classifier in a weakly-supervised manner. Concretely, we employed Hinge loss in the contrastive learning component to amplify the dissimilarity between ID and OOD pairs. In addition, we developed a Feature Sparsity Regularizer to selectively incorporate crucial features from data of two modalities for the binary classifier. We also devised a novel scoring metric to effectively fuse predictions from both components. The evaluation results validated that the proposed hybrid approach excels in identifying anomalies across three different OOD scenarios. Our future work will focus on applying the proposed WOOD to more OOD scenarios to better represent the wide spectrum of OOD environments in the real world.

References

Daniel Bogdoll, Maximilian Nitsche, and J Marius Zöllner. Anomaly detection in autonomous driving: A survey. In *Proceedings of the IEEE/CVF Conference on Computer Vision and Pattern Recognition*, pp. 4488–4499, 2022.

Thomas Davenport and Ravi Kalakota. The potential for artificial intelligence in healthcare. *Future healthcare journal*, 6(2):94, 2019.

Dina Demner-Fushman, Marc D Kohli, Marc B Rosenman, Sonya E Shooshan, Laritza Rodriguez, Sameer Antani, George R Thoma, and Clement J McDonald. Preparing a collection of radiology examinations for distribution and retrieval. *Journal of the American Medical Informatics Association*, 23(2):304–310, 2016.

Terrance DeVries and Graham W Taylor. Learning confidence for out-of-distribution detection in neural networks. *arXiv preprint arXiv:1802.04865*, 2018.

Xuefeng Du, Xin Wang, Gabriel Gozum, and Yixuan Li. Unknown-aware object detection: Learning what you don't know from videos in the wild. In *Proceedings of the IEEE/CVF Conference on Computer Vision and Pattern Recognition*, pp. 13678–13688, 2022.

Sepideh Esmaeilpour, Bing Liu, Eric Robertson, and Lei Shu. Zero-shot out-of-distribution detection based on the pretrained model clip. In *Proceedings of the AAAI conference on artificial intelligence*, 2022.

Stanislav Fort, Jie Ren, and Balaji Lakshminarayanan. Exploring the limits of out-of-distribution detection. *Advances in Neural Information Processing Systems*, 34:7068–7081, 2021.

Mariana-Iuliana Georgescu, Antonio Barbalau, Radu Tudor Ionescu, Fahad Shahbaz Khan, Marius Popescu, and Mubarak Shah. Anomaly detection in video via self-supervised and multi-task learning. In *Proceedings of the IEEE/CVF conference on computer vision and pattern recognition*, pp. 12742–12752, 2021.

Changhee Han, Leonardo Rundo, Kohei Murao, Takafumi Nemoto, and Hideki Nakayama. Bridging the gap between ai and healthcare sides: towards developing clinically relevant ai-powered diagnosis systems. In *IFIP International Conference on Artificial Intelligence Applications and Innovations*, pp. 320–333. Springer, 2020.

Zongbo Han, Fan Yang, Junzhou Huang, Changqing Zhang, and Jianhua Yao. Multimodal dynamics: Dynamical fusion for trustworthy multimodal classification. In *Proceedings of the IEEE/CVF Conference on Computer Vision and Pattern Recognition*, pp. 20707–20717, 2022.

Matthias Hein, Maksym Andriushchenko, and Julian Bitterwolf. Why relu networks yield high-confidence predictions far away from the training data and how to mitigate the problem. In *Proceedings of the IEEE/CVF Conference on Computer Vision and Pattern Recognition*, pp. 41–50, 2019.

Dan Hendrycks and Kevin Gimpel. A baseline for detecting misclassified and out-of-distribution examples in neural networks. *arXiv preprint arXiv:1610.02136*, 2016.

Dan Hendrycks and Kevin Gimpel. A baseline for detecting misclassified and out-of-distribution examples in neural networks. In *International Conference on Learning Representations*, 2017.

Dan Hendrycks, Mantas Mazeika, and Thomas Dietterich. Deep anomaly detection with outlier exposure. *arXiv preprint arXiv:1812.04606*, 2018.

Rui Huang and Yixuan Li. Mos: Towards scaling out-of-distribution detection for large semantic space. In *Proceedings of the IEEE/CVF Conference on Computer Vision and Pattern Recognition*, pp. 8710–8719, 2021.

Rasheed Hussain and Sherali Zeadally. Autonomous cars: Research results, issues, and future challenges. *IEEE Communications Surveys & Tutorials*, 21(2):1275–1313, 2018.

Tianchen Ji, Sri Theja Vuppala, Girish Chowdhary, and Katherine Driggs-Campbell. Multi-modal anomaly detection for unstructured and uncertain environments. *arXiv preprint arXiv:2012.08637*, 2020.

Qian Jiang, Changyou Chen, Han Zhao, Liqun Chen, Qing Ping, Son Dinh Tran, Yi Xu, Belinda Zeng, and Trishul Chilimbi. Understanding and constructing latent modality structures in multi-modal representation learning. In *Proceedings of the IEEE/CVF Conference on Computer Vision and Pattern Recognition*, pp. 7661–7671, 2023.

Alistair EW Johnson, Tom J Pollard, Seth J Berkowitz, Nathaniel R Greenbaum, Matthew P Lungren, Chih-ying Deng, Roger G Mark, and Steven Horng. Mimic-cxr, a de-identified publicly available database of chest radiographs with free-text reports. *Scientific data*, 6(1):1–8, 2019.

Ramneet Kaur, Kaustubh Sridhar, Sangdon Park, Susmit Jha, Anirban Roy, Oleg Sokolsky, and Insup Lee. Codit: Conformal out-of-distribution detection in time-series data. *arXiv preprint arXiv:2207.11769*, 2022.

Diederik P Kingma and Jimmy Ba. Adam: A method for stochastic optimization. *arXiv preprint arXiv:1412.6980*, 2014.

Daoheng Li, Xiushan Nie, Xiaofeng Li, Yu Zhang, and Yilong Yin. Context-related video anomaly detection via generative adversarial network. *Pattern Recognition Letters*, 156:183–189, 2022a.

Yewen Li, Chaojie Wang, Xiaobo Xia, Tongliang Liu, Xin Miao, and Bo An. Out-of-distribution detection with an adaptive likelihood ratio on informative hierarchical vae. In *Advances in Neural Information Processing Systems*, 2022b.

Tsung-Yi Lin, Michael Maire, Serge Belongie, James Hays, Pietro Perona, Deva Ramanan, Piotr Dollár, and C Lawrence Zitnick. Microsoft coco: Common objects in context. In *European conference on computer vision*, pp. 740–755. Springer, 2014.

Weitang Liu, Xiaoyun Wang, John Owens, and Yixuan Li. Energy-based out-of-distribution detection. *Advances in Neural Information Processing Systems*, 33:21464–21475, 2020.

Philipp Liznerski, Lukas Ruff, Robert A Vandermeulen, Billy Joe Franks, Klaus-Robert Müller, and Marius Kloft. Exposing outlier exposure: What can be learned from few, one, and zero outlier images. *arXiv preprint arXiv:2205.11474*, 2022.

Xiaoxiao Ma, Jia Wu, Shan Xue, Jian Yang, Chuan Zhou, Quan Z Sheng, Hui Xiong, and Leman Akoglu. A comprehensive survey on graph anomaly detection with deep learning. *IEEE Transactions on Knowledge and Data Engineering*, 2021.

Samual MacDonald, Kaiah Steven, and Maciej Trzaskowski. Interpretable ai in healthcare: Enhancing fairness, safety, and trust. In *Artificial Intelligence in Medicine*, pp. 241–258. Springer, 2022.

Snehashis Majhi, Srijan Das, François Brémond, Ratnakar Dash, and Pankaj Kumar Sa. Weakly-supervised joint anomaly detection and classification. In *2021 16th IEEE International Conference on Automatic Face and Gesture Recognition (FG 2021)*, pp. 1–7. IEEE, 2021.

Yifei Ming, Ziyang Cai, Jiuxiang Gu, Yiyou Sun, Wei Li, and Yixuan Li. Delving into out-of-distribution detection with vision-language representations. In *Advances in Neural Information Processing Systems*, 2022a.

Yifei Ming, Ziyang Cai, Jiuxiang Gu, Yiyou Sun, Wei Li, and Yixuan Li. Delving into out-of-distribution detection with vision-language representations. In *Advances in Neural Information Processing Systems*, 2022b.

Yifei Ming, Ying Fan, and Yixuan Li. Poem: Out-of-distribution detection with posterior sampling. In *International Conference on Machine Learning*, pp. 15650–15665. PMLR, 2022c.

Atsuyuki Miyai, Qing Yu, Go Irie, and Kiyoharu Aizawa. Zero-shot in-distribution detection in multi-object settings using vision-language foundation models. *arXiv preprint arXiv:2304.04521*, 2023.

Atsuyuki Miyai, Qing Yu, Go Irie, and Kiyoharu Aizawa. Locoop: Few-shot out-of-distribution detection via prompt learning. *Advances in Neural Information Processing Systems*, 36, 2024.

Vivek Narayanaswamy, Yamen Mubarka, Rushil Anirudh, Deepta Rajan, Andreas Spanias, and Jayaraman J Thiagarajan. Know your space: Inlier and outlier construction for calibrating medical ood detectors. In *Medical Imaging with Deep Learning*, 2023.

Alexander Podolskiy, Dmitry Lipin, Andrey Bout, Ekaterina Artemova, and Irina Piontkovskaya. Revisiting mahalanobis distance for transformer-based out-of-domain detection. In *Proceedings of the AAAI Conference on Artificial Intelligence*, volume 35, pp. 13675–13682, 2021.

Yuning Qiu, Teruhisa Misu, and Carlos Busso. Unsupervised scalable multimodal driving anomaly detection. *IEEE Transactions on Intelligent Vehicles*, 2022.

Alec Radford, Jong Wook Kim, Chris Hallacy, Aditya Ramesh, Gabriel Goh, Sandhini Agarwal, Girish Sastry, Amanda Askell, Pamela Mishkin, Jack Clark, et al. Learning transferable visual models from natural language supervision. In *International Conference on Machine Learning*, pp. 8748–8763. PMLR, 2021.

Scott Reed, Zeynep Akata, Honglak Lee, and Bernt Schiele. Learning deep representations of fine-grained visual descriptions. In *Proceedings of the IEEE conference on computer vision and pattern recognition*, pp. 49–58, 2016.

Jie Ren, Stanislav Fort, Jeremiah Liu, Abhijit Guha Roy, Shreyas Padhy, and Balaji Lakshminarayanan. A simple fix to mahalanobis distance for improving near-ood detection. *arXiv preprint arXiv:2106.09022*, 2021.

Mauricio Romero and Pablo A Estévez. Outlier detection based on transformations for astronomical time series. In *2022 International Joint Conference on Neural Networks (IJCNN)*, pp. 1–8. IEEE, 2022.

Abhijit Guha Roy, Jie Ren, Shekoofeh Azizi, Aaron Loh, Vivek Natarajan, Basil Mustafa, Nick Pawlowski, Jan Freyberg, Yuan Liu, Zach Beaver, et al. Does your dermatology classifier know what it doesn't know? detecting the long-tail of unseen conditions. *Medical Image Analysis*, 75:102274, 2022.

Lukas Ruff, Jacob R Kauffmann, Robert A Vandermeulen, Grégoire Montavon, Wojciech Samek, Marius Kloft, Thomas G Dietterich, and Klaus-Robert Müller. A unifying review of deep and shallow anomaly detection. *Proceedings of the IEEE*, 109(5):756–795, 2021.

Mohammadreza Salehi, Hossein Mirzaei, Dan Hendrycks, Yixuan Li, Mohammad Hossein Rohban, and Mohammad Sabokrou. A unified survey on anomaly, novelty, open-set, and out of-distribution detection: Solutions and future challenges. *Transactions of Machine Learning Research*, 2022.

Piyush Sharma, Nan Ding, Sebastian Goodman, and Radu Soricut. Conceptual captions: A cleaned, hypernymed, image alt-text dataset for automatic image captioning. In *Proceedings of the 56th Annual Meeting of the Association for Computational Linguistics (Volume 1: Long Papers)*, pp. 2556–2565, 2018.

Waqas Sultani, Chen Chen, and Mubarak Shah. Real-world anomaly detection in surveillance videos. In *Proceedings of the IEEE conference on computer vision and pattern recognition*, pp. 6479–6488, 2018.

Lei Sun, Kailun Yang, Xinxin Hu, Weijian Hu, and Kaiwei Wang. Real-time fusion network for rgb-d semantic segmentation incorporating unexpected obstacle detection for road-driving images. *IEEE Robotics and Automation Letters*, 5(4):5558–5565, 2020.

Yiyou Sun and Yixuan Li. Dice: Leveraging sparsification for out-of-distribution detection. In *Computer Vision–ECCV 2022: 17th European Conference, Tel Aviv, Israel, October 23–27, 2022, Proceedings, Part XXIV*, pp. 691–708. Springer, 2022.

Yiyou Sun, Chuan Guo, and Yixuan Li. React: Out-of-distribution detection with rectified activations. *Advances in Neural Information Processing Systems*, 34:144–157, 2021.

Yiyou Sun, Yifei Ming, Xiaojin Zhu, and Yixuan Li. Out-of-distribution detection with deep nearest neighbors. In *International Conference on Machine Learning*, 2022.

Leitian Tao, Xuefeng Du, Xiaojin Zhu, and Yixuan Li. Non-parametric outlier synthesis. *arXiv preprint arXiv:2303.02966*, 2023.

Engkarat Techapanurak, Masanori Suganuma, and Takayuki Okatani. Hyperparameter-free out-of-distribution detection using cosine similarity. In *Proceedings of the Asian conference on computer vision*, 2020.

Yu Tian, Gabriel Maicas, Leonardo Zorron Cheng Tao Pu, Rajvinder Singh, Johan W Verjans, and Gustavo Carneiro. Few-shot anomaly detection for polyp frames from colonoscopy. In *International Conference on Medical Image Computing and Computer-Assisted Intervention*, pp. 274–284. Springer, 2020.

Joost Van Amersfoort, Lewis Smith, Yee Whye Teh, and Yarin Gal. Uncertainty estimation using a single deep deterministic neural network. In *International conference on machine learning*, pp. 9690–9700. PMLR, 2020.

Catherine Wah, Steve Branson, Peter Welinder, Pietro Perona, and Serge Belongie. The caltech-ucsd birds-200-2011 dataset. 2011.

Fengjun Wang, Sarai Mizrachi, Moran Beladev, Guy Nadav, Gil Amsalem, Karen Lastmann Assaraf, and Hadas Harush Boker. Mumic–multimodal embedding for multi-label image classification with tempered sigmoid. In *Proceedings of the AAAI Conference on Artificial Intelligence*, volume 37, pp. 15603–15611, 2023a.

Hualiang Wang, Yi Li, Huifeng Yao, and Xiaomeng Li. Clipn for zero-shot ood detection: Teaching clip to say no. In *Proceedings of the IEEE/CVF International Conference on Computer Vision*, pp. 1802–1812, 2023b.

Jun Wang, Li Zhang, Yanjun Huang, and Jian Zhao. Safety of autonomous vehicles. *Journal of advanced transportation*, 2020, 2020.

LeiChen Wang, Simon Giebenhain, Carsten Anklam, and Bastian Goldluecke. Radar ghost target detection via multimodal transformers. *IEEE Robotics and Automation Letters*, 6(4):7758–7765, 2021.

Lin Wang, Fuqiang Zhou, Zuoxin Li, Wangxia Zuo, and Haishu Tan. Abnormal event detection in videos using hybrid spatio-temporal autoencoder. In *2018 25th IEEE International Conference on Image Processing (ICIP)*, pp. 2276–2280. IEEE, 2018.

Zhisheng Xiao, Qing Yan, and Yali Amit. Likelihood regret: An out-of-distribution detection score for variational auto-encoder. *Advances in neural information processing systems*, 33:20685–20696, 2020.

Jingkang Yang, Kaiyang Zhou, Yixuan Li, and Ziwei Liu. Generalized out-of-distribution detection: A survey. *arXiv preprint arXiv:2110.11334*, 2021.

Karina Zadorozhny, Patrick Thoral, Paul Elbers, and Giovanni Cinà. Out-of-distribution detection for medical applications: Guidelines for practical evaluation. In *Multimodal AI in healthcare: A paradigm shift in health intelligence*, pp. 137–153. Springer, 2022.

Alireza Zaeemzadeh, Niccolo Bisagno, Zeno Sambugaro, Nicola Conci, Nazanin Rahnavard, and Mubarak Shah. Out-of-distribution detection using union of 1-dimensional subspaces. In *Proceedings of the IEEE/CVF Conference on Computer Vision and Pattern Recognition*, pp. 9452–9461, 2021.

Li Ming Zhan, Haowen Liang, Bo Liu, Lu Fan, Xiao Ming Wu, and Albert YS Lam. Out-of-scope intent detection with self-supervision and discriminative training. In *Joint Conference of the 59th Annual Meeting of the Association for Computational Linguistics and the 11th International Joint Conference on Natural Language Processing, ACL-IJCNLP 2021*, pp. 3521–3532. Association for Computational Linguistics (ACL), 2021.

Kaiyang Zhou, Jingkang Yang, Chen Change Loy, and Ziwei Liu. Conditional prompt learning for vision-language models. In *Proceedings of the IEEE/CVF Conference on Computer Vision and Pattern Recognition*, pp. 16816–16825, 2022a.

Wenxuan Zhou, Fangyu Liu, and Muhao Chen. Contrastive out-of-distribution detection for pretrained transformers. *arXiv preprint arXiv:2104.08812*, 2021.

Yunhua Zhou, Peiju Liu, and Xipeng Qiu. Knn-contrastive learning for out-of-domain intent classification. In *Proceedings of the 60th Annual Meeting of the Association for Computational Linguistics (Volume 1: Long Papers)*, pp. 5129–5141, 2022b.